BRNO UNIVERSITY OF TECHNOLOGY
VYSOKÉ UČENÍ TECHNICKÉ V BRNĚ

FACULTY OF MECHANICAL ENGINEERING
INSTITUTE OF PHYSICAL ENGINEERING

FAKULTA STROJNÍHO INŽENÝRSTVÍ
ÚSTAV FYZIKÁLNÍHO INŽENÝRSTVÍ

MATERIALS AND THEIR APPLICATION IN LOW TEMPERATURE PARTS OF STM MICROSCOPE

BACHELOR'S THESIS
BAKALÁŘSKÁ PRÁCE

AUTHOR JAKUB VOŇKA
AUTOR PRÁCE

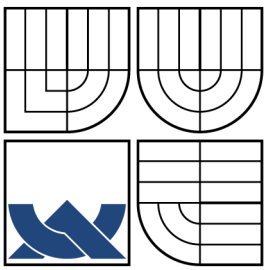

BRNO UNIVERSITY OF TECHNOLOGY
VYSOKÉ UČENÍ TECHNICKÉ V BRNĚ

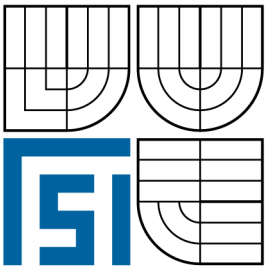

FACULTY OF MECHANICAL ENGINEERING
INSTITUTE OF PHYSICAL ENGINEERING

FAKULTA STROJNÍHO INŽENÝRSTVÍ
ÚSTAV FYZIKÁLNÍHO INŽENÝRSTVÍ

MATERIALS AND THEIR APPLICATION IN LOW TEMPERATURE PARTS OF STM MICROSCOPE

MATERIÁLY A JEJICH APLIKACE V NÍZKOTEPLOTNÍCH ČÁSTECH STM MIKROSKOPU

BACHELOR'S THESIS
BAKALÁŘSKÁ PRÁCE

AUTHOR
AUTOR PRÁCE
JAKUB VOŇKA

SUPERVISOR
VEDOUCÍ PRÁCE
Ing. PAVEL URBAN, Ph.D.

BRNO 2011

This bachelor's thesis was elaborated at the

Institute of Scientific Instruments of the AS CR, v. v. i.

within the frame of the Contract of scientific collaboration, No: 0313220 03950,
between
the Institute of Scientific Instruments of the AS CR, v. v. i.
and
the Faculty of Mechanical Engineering of Brno University of Technology.

under supervision of:
Ing. Pavel Urban, Ph.D.

Vysoké učení technické v Brně, Fakulta strojního inženýrství

Ústav fyzikálního inženýrství
Akademický rok: 2010/2011

ZADÁNÍ BAKALÁŘSKÉ PRÁCE

student(ka): Jakub Voňka

který/která studuje v **bakalářském studijním programu**

obor: **Fyzikální inženýrství a nanotechnologie (3901R043)**

Ředitel ústavu Vám v souladu se zákonem č.111/1998 o vysokých školách a se Studijním a zkušebním řádem VUT v Brně určuje následující téma bakalářské práce:

Materiály a jejich aplikace v nízkoteplotních částech STM mikroskopu

v anglickém jazyce:

Materials and their application in low temperature parts of STM microscope

Stručná charakteristika problematiky úkolu:

Pro účely návrhu nízkoteplotního UHV-STM mikroskopu na Ústavu fyzikálního inženýrství je potřebné nalézt materiály s vhodnými tepelnými a mechanickými vlastnostmi. K ochlazení studovaných vzorků bude použito průtokové chlazení kapalným He (~ 4.2 K). Výběr materiálů je významný zejména z důvodu minimalizace parazitních tepelných toků k nízkoteplotním částem mikroskopu (tepelně izolační materiály), odvedení tepelné zátěže vzorku (materiály s vysokou tepelnou vodivostí), vakuové kompatibility (nízká hodnota odplynění ve vakuu), dostatečné tuhosti (minimalizace vlivu vibrací). Správná volba materiálů a jejich aplikace má umožnit dosáhnout nízké teploty studovaných vzorků (~ 25 K) a hospodárný provozu mikroskopu s nízkou spotřebou He.

Cíle bakalářské práce:

Cílem práce je výběr vhodných materiálů s ohledem na jejich tepelné a mechanické vlastnosti a jejich aplikace v klíčových součástech nízkoteplotního UHV-STM. Pro posouzení správné volby materiálů provést rozbor dostupné literatury, nezbytné výpočty a měření jejich vlastností, zejména tepelné vodivosti.

ABSTRACT

Cryogenic flow cryostat with liquid helium (LHe) is being developed by Group of Cryogenics and Superconductivity at Institute of Scientific Instruments for the existing scanning tunneling microscope (STM) working at ambient temperature at Institute of Physical Engineering. This thesis deals with the selection of materials and determination of their material characteristics for potential use in some parts of the low temperature STM (LT-STM), focusing mostly on thermal conductivity in temperature range from $4\,\mathrm{K}$ to $300\,\mathrm{K}$. Problematics of copper braids for thermal connection of the sample with cold heat exchanger is discussed. CuCrZr alloy was closely studied as a possible material for sample holder. Heat fluxes through low conductive supports based on thermal resistance of spherical contacts were determined for possible use as an insulation between cold sample holder and STM table.

KEYWORDS

thermal conductivity, flow LHe cryostat, STM, cryogenics

ABSTRAKT

Průtokový kryostat s kapalným héliem (LHe) je vyvíjen skupinou Kryogeniky a Supravodivosti na Ústavu Přístrojové Techniky pro stávající rastrovací tunelovací mikroskop (STM) pracující za pokojové teploty na Ústavu Fyzikálního Inženýrství. Tato bakalářská práce se zabýva výběrem materiálů a určením jejich vlastností pro potenciální využití v některých částech nízkoteplotního STM mikroskopu (LT-STM), se zaměřením zejména na tepelnou vodivost v teplotním rozsahu od $4\,\mathrm{K}$ do $300\,\mathrm{K}$. Je zde probírána problematika měděných svazků pro tepelné spojení vzorku s tepelným výměníkem. Slitina CuCrZr byla podrobně zkoumána jako vhodný materiál pro držák vzorku. Byly určeny tepelné toky málo vodivými podpěrami založenými na styku sférických ploch pro použití jako izolace mezi studeným držákem vzorku a STM stolkem.

KLÍČOVÁ SLOVA

tepelná vodivost, průtokový LHe kryostat, STM, kryogenika

VOŇKA, Jakub *Materials and their application in low temperature parts of STM microscope*: bachelor's thesis. Brno: Brno University of Technology, Faculty of Mechanical Engineering, Institute of Physical Engineering, 2011. 39 p. Supervised by Ing. Pavel Urban, Ph.D.

DECLARATION

I declare that I have elaborated my bachelor's thesis on the theme of "Materials and their application in low temperature parts of STM microscope" independently, under the supervision of the bachelor's thesis supervisor and with the use of technical literature and other sources of information which are all quoted in the thesis and detailed in the list of literature at the end of the thesis.

As the author of the bachelor's thesis I furthermore declare that, concerning the creation of this bachelor's thesis, I have not infringed any copyright. In particular, I have not unlawfully encroached on anyone's personal copyright and I am fully aware of the consequences in the case of breaking Regulation § 11 and the following of the Copyright Act No 121/2000 Vol., including the possible consequences of criminal law resulted from Regulation § 152 of Criminal Act No 140/1961 Vol.

Brno ....

(author's signature)

ACKNOWLEDGMENTS

I would like to express my thanks to Ing. Pavel Hanzelka and Ing. Pavel Urban Ph.D. for guiding this thesis and many valuable insights, whole Group of Cryogenics and Superconductivity for pleasant and originative environment, and my parents for their loving support.

CONTENTS

LIST OF FIGURES

LIST OF TABLES

INTRODUCTION

This thesis deals with the selection of materials for potential use in some parts of the low temperature scanning tunneling microscope (LT-STM), focusing mostly on thermal conductivity. The flow cryogenic cooling system with liquid helium (LHe) is designed by Group of Cryogenics and Superconductivity at the Institute of Scientific Instruments. The system will be used for the existing STM [1] working at room temperatures at the Institute of Physical Engineering at Brno University of Technology. The STM table with cryogenic cooling is schematically shown in Fig. 1.

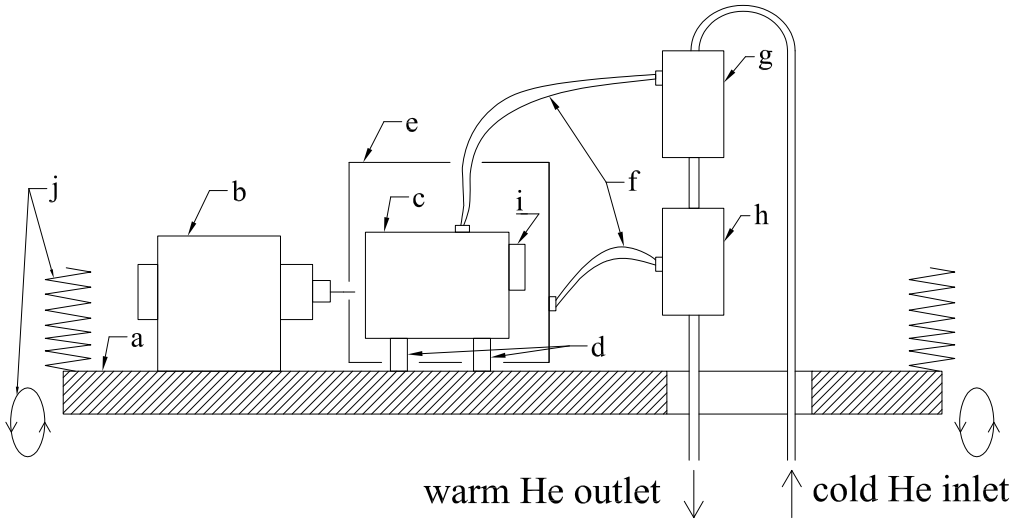

Fig. 1: Schematic representation of LT-STM apparatus. Scheme shows: (a) LT-STM table, (b) scanning head, (c) sample holder, (d) low conductivity supports, (e) radiative shield, (f) copper braids, (g) colder heat exchanger, (h) hotter heat exchanger, (i) heater, (j) spring and electromagnetic damping.

On the table isolated from vibrations via springs and electromagnetic damping there is a scanning head and a cold sample holder. The holder is thermally connected to the colder heat exchanger via copper braid. The heat exchangers are part of the He circuit. He enters the first heat exchanger at about 5 K, where it warms up. Warmed He enters the second heat exchanger at about 50 K, warms up even more and leaves the system through the output line. The second heat exchanger with the braid cools the radiative shield at about 60 K around the sample holder. The shield lowers the radiative heat transfer to the sample holder significantly and is necessary to achieve low temperature of the holder. To prevent massive heat load to the sample holder by heat conduction from the table, the sample is placed on low conductivity supports.

One part of the thesis is devoted to copper braids used for thermal connection of the cooled parts with cold heat exchangers. Thermal conductivity of such braids

was studied to determine their right thickness for conducting enough cooling power and ensure small temperature drop between sample holder and heat exchanger. In the next part a CuCrZr alloy was closely studied for its good mechanical strength and relatively high thermal conductivity. Such material characteristics are needed for example for the sample holder or heat exchangers. The last part of the thesis deals with the thermal isolation of the cold sample holder from the table at ambient temperature. Thermal conductivity of a support with glass spheres in contact was studied both theoretically and experimentally.

This bachelor's thesis was elaborated at the Institute of Scientific Instruments of the AS CR, v. v. i. within the frame of the Contract of scientific collaboration, No: 0313220 03950, between the Institute of Scientific Instruments of the AS CR, v. v. i. and the Faculty of Mechanical Engineering of Brno University of Technology. Experimental work was done in collaboration with Group of Cryogenics and Superconductivity.

1 THEORY

1.1 Thermal conductivity

1.1.1 Definition of thermal conductivity

The conduction heat flux[1] Q through a small element of solid bar is given by

$$Q = \lambda(T) S \frac{\mathrm{d}T}{\mathrm{d}x}, \tag{1.1}$$

where S is a cross-sectional area, $\frac{\mathrm{d}T}{\mathrm{d}x}$ is the temperature gradient along the element and $\lambda(T)$ it the temperature-dependent thermal conductivity describing the ability of the material to conduct heat [2]. For the typical situation with constant cross-sectional area along the whole length L of the bar, Eq. 1.1 can be integrated to obtain

$$Q = \frac{S}{L} \int_{T_A}^{T_B} \lambda\left(T\right) dT. \tag{1.2}$$

Since $\lambda(T)$ has frequently very strong dependence on temperature, an analytical solution of the integral from Eq. 1.2 is often not convenient to use. For that reason so called *integral thermal conductivity* $\Lambda\left(T_A, T_B\right)$ is used [3]

$$\Lambda\left(T_A, T_B\right) = \int_{T_A}^{T_B} \lambda\left(T\right) dT. \tag{1.3}$$

Its values for various materials between given temperatures are tabulated, for most cryogenic applications referring to boiling point of ^{4}He: T_0=4.2 K. We can use the following relation to determine values of Λ to any reference temperature

$$\int_{T_A}^{T_B} \lambda\left(T\right) dT = \int_{T_0}^{T_B} \lambda\left(T\right) dT - \int_{T_0}^{T_A} \lambda\left(T\right) dT \tag{1.4}$$

$$\Lambda\left(T_A, T_B\right) = \Lambda\left(T_0, T_B\right) - \Lambda\left(T_0, T_A\right) \tag{1.5}$$

for $T_0 < T_A < T_B$.

1.1.2 Mechanisms of thermal conductivity

For all solids, one mechanism for energy transport is associated with thermal vibrations moving through a material [4]. By analogy with particle energy transfer

[1] This notation may seem odd, but in cryogenics the most of the calculations are not based on quantities of heat in the system, but heat fluxes. Hence the symbol Q for heat flux is used for convenience.

these vibrational waves can be treated as particles, called *phonons*. Energy transport connected with vibrations is called *phonon conduction*. This is the dominant conduction mechanism in electrical insulators.

In metals that are good electrical conductors (i.e., copper, gold), energy transfer involves two mechanisms: (1) phonon energy transport and (2) electron energy transport. These two mechanisms act in parallel and the total thermal conductivity is a sum of contributions resulting from the phonons and resulting from the electrons. There is relatively large number of conduction electrons in metals, thus the electron contribution is usually the larger component of heat conduction. The electron conduction is influenced by two major scattering processes: (1) scattering on phonons and (2) scattering on the imperfections of the lattice. With lowering the temperature the vibrations of lattice become smaller, i.e., there are less phonons. Hence, the phonon energy transfer and phonon scattering becomes negligible. That results in rising of the thermal conductivity to its maximum (e.g., about 20 K for copper, see Fig. 1.1). Lowering the temperature even more results in lowering the thermal conductivity. This is due to the fact that the scattering processes and number of conducting electrons are constant, but heat capacity of the electrons is lowering with temperature. Thermal conductivity of some common cryogenic materials are shown in Fig. 1.1.

1.2 Electrical Conductivity

Measuring the electrical conductivity is, in general, much easier than direct measurement of the low temperature thermal conductivity. Fortunately, thanks to the fact that in metals both conductivities have one common transfer mechanism (electron transport), measuring the electrical conductivity and application of the Wiedeman-Franz-Lorentz law often gives a reasonable information about thermal conductivity.

1.2.1 Wiedeman-Franz-Lorentz Law

For the electrical conductivity, the electrons transport charge which is temperature independent. Thus at low temperatures under about 20 K, where phonon scattering is not significant and scattering at lattice imperfections is temperature independent, the electrical conductivity σ does not depend on temperature. For the thermal conductivity electrons carry heat, but their heat capacity is proportional to temperature at these temperatures. Therefore, the ratio of thermal conductivity λ to electrical conductivity σ is proportional to temperature. This is expressed by the

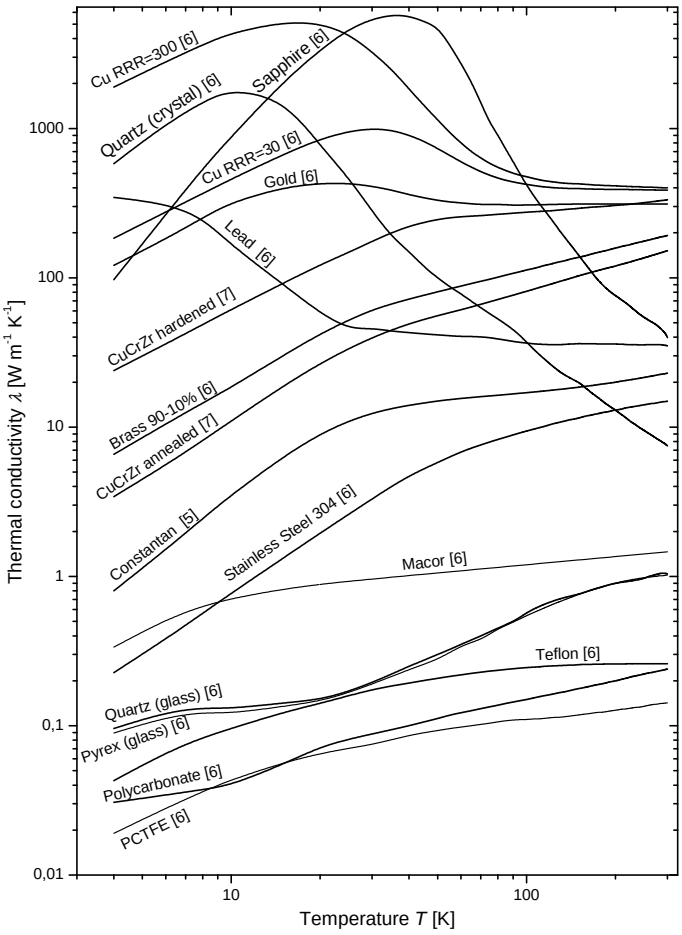

Fig. 1.1: Thermal conductivity of some common cryogenic materials

Wiedeman-Franz-Lorentz law [4]

$$\frac{\lambda}{\sigma} = L_0 T, \tag{1.6}$$

where L_0 is a Lorentz number equal to

$$L_0 = \frac{\pi^2}{3}\left(\frac{k_\mathrm{B}}{e}\right)^2 = 2.44 \times 10^{-8}\,\mathrm{W\,\Omega\,K^{-2}}, \tag{1.7}$$

where k_B is the Boltzman constant and e is an elementary charge. Measured electrical conductivity can be used together with the Wiedeman-Franz-Lorentz law to determine thermal conductivity of a metal.

For metals, this method gives reasonably accurate results at temperatures significantly lower than Debeye temperature T_Θ (e.g. $T_\Theta = 315\,\mathrm{K}$ for copper) and at temperatures higher than T_Θ. In the temperature range between, the law is not accurate enough due to non-elastic electron-phonon collisions [8].

1.2.2 Residual Resistance Ratio

Especially in copper, but in other metals as well, there is a very strong dependence of thermal conductivity on purity and condition of a metal. The conductivity can vary over several orders of magnitude even for the same metal. To describe the purity of a metal, a characteristic dimensionless constant RRR (Residual Resistance Ratio) is often used [2]. It is defined as a ratio of the electrical resistance at room temperature[2] (298 K) to the resistance at the temperature of boiling point of helium at normal pressure (4.2 K).

$$\mathrm{RRR} = \frac{\rho_{298\,\mathrm{K}}}{\rho_{4.2\,\mathrm{K}}} \tag{1.8}$$

RRR is a measure of scattering on defects. It indicates how pure the material is by showing how much does the conductivity increase with eliminating the influence of electron-phonon scattering. For copper the usual values of RRR vary from 10 to about 1000. Naturally, higher the value of RRR higher the purity and conductivity of a metal.

1.2.3 Predicting thermal conductivity from RRR

Hust et al. [9] presented a set of semi-empirical equations which can be used to describe the thermal conductivity of pure metals from low temperatures to room temperature and above. From these equations a method of calculation of thermal conductivity from RRR value can be derived and is used by software Cryocomp [6]. This method is applicable to samples with RRR values from 10 to 10 000.

For copper and especially aluminum precipitation hardened alloys Woodcraft [10] modified the equations given by Hust et al. [9] by altering the term describing the strength of the electron-phonon interaction from a constant to a function of the alloy purity. He also developed a program for calculation of the thermal conductivity with these modified equations, which is freely available [11]. He states that this method extends the lower limit of validity from approximately RRR = 10 to RRR > 2.

1.3 Contact Mechanics

Calculation of heat fluxes through the contact of spherical bodies incorporated in supports, discussed in chapter 4, requires a knowledge of mechanical contact area. Hence, the basics of the contact mechanics should be introduced.

The theory was developed by Heinrich Hertz and applies to normal contact between two smooth elastic solids that can be described locally with radii of curvature [12]. The size of the contact area must be small compared to the dimension

[2] Some authors use the temperature of a triple point of water at normal pressure (273 K).

of the bodies in contact and to the radii of curvature. Hertz assumed, that the stress exerted by a sphere follows an elliptical distribution, see Fig. 1.2. Based on this assumption he developed a model for the calculation of contact areas and stress distribution.

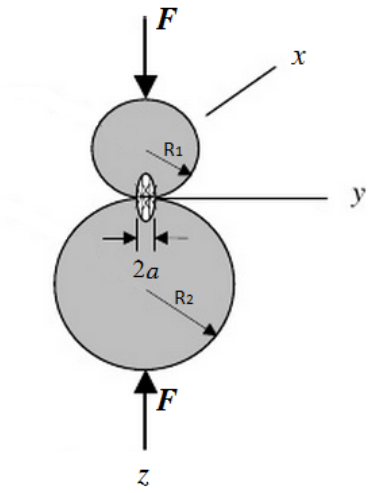

Fig. 1.2: Two spherical bodies in contact. An elliptical distribution of stress in contact area with diameter $2a$ is shown [12].

Equations (1.9) to (1.12) are Hertz equations for circular contact of two spheres. For the calculation it is convenient to introduce the contact modulus E and relative radius R. The contact modulus expresses the elastic properties of both bodies. The relative radius is a sum of inverse radii. The curvature is positive for convex surface and negative for concave surface.

$$\frac{1}{E} = \frac{1-\nu_1^2}{E_1} + \frac{1-\nu_2^2}{E_2} \tag{1.9}$$

$$\frac{1}{R} = \frac{1}{R_1} + \frac{1}{R_2} \tag{1.10}$$

E_1 and E_2 are Young's moduli of elasticity, ν_1 and ν_2 are Poisson's ratios of the solids. R_1 and R_2 are the radii of the spheres. Using equations (1.9) and (1.10) the contact area radius a and maximum pressure $p_{\max}$ can be calculated

$$a = \left(\frac{3FR}{4E}\right)^{\frac{1}{3}} \tag{1.11}$$

$$p_{\max} = \frac{3F}{2\pi a^2}, \tag{1.12}$$

where F is the mechanical load (Fig. 1.2). The topic is described in more detail for example in [13].

2 COPPER BRAIDS

2.1 Introduction

Boiling cryogen in a heat exchanger is a source of strong vibrations that could degrade the performance of the STM. Typically, the cooling of a sample is achieved by linkage between a cold heat exchanger and the sample holder by a bundle of thin high conductivity copper wires so called *braid*. Thicker the braid, more adverse vibrations are transfered through [1]. On the other hand for bringing enough cooling power, adequate thickness is necessary. Thus, a compromise has to be found.

For our LT-STM design two copper braids were coming into consideration. One used at the Institute of Physical Engineering (further just *IPE braid*) and the other one at the Institute of Scientific Instruments (further just *ISI braid*). Proper measurement of the thermal conductivity of both braids was needed to determine which braid is more suitable for this design and how thick does it have to be.

2.2 Thermal conductivity determination from electrical resistivity

2.2.1 Description

By measuring electrical resistivity it is possible to determine thermal conductivity using RRR value of a material and Wiedeman-Franz-Lorentz Law (see section 1.2.3). For this reason RRR was measured and thermal conductivity was determined at different temperatures using software Cryocomp [6]. This program calculates various physical characteristics of more than 60 materials in a temperature range from 1 K to 300 K. RRR was measured on two samples of IPE braid (marked IPE 1 and IPE 2) and also two samples of ISI braid (marked ISI 1 and ISI 2). The values of the electrical resistance of braids, especially at 4 K, are small, thus the resistance was measured in four-wire circuit. Electrical resistance and thermal conductivity are very dependent on the mechanical deformation of a sample. To lower the effect of the deformations, one sample of IPE braid (marked IPE 1) and one sample of ISI braid (marked ISI 1) was annealed at 700°C. He atmosphere was used during annealing to prevent oxidation.

2.2.2 Results

RRR of braids was determined to be about 53 for IPE braid and around 63 for ISI braid. No significant difference in measured RRR on annealed and not annealed

samples was found. Final values of RRR measurement are in Tab. 2.1. The calculated values of thermal conductivity for various RRR is plotted together with measured data for ISI 1 braid in Fig. 2.2.

Tab. 2.1: Table of measured RRR values of copper braids

Braid marking	**Annealing**	**Diameter** $[\mu m]$	**Lenght** $[mm]$	**RRR** $[\,-\,]$
ISI 1	✓	75	77	63.9
ISI 2		63	94	62.5
IPE 1	✓	190	94	52.6
IPE 2		190	82	54.1

2.3 Direct measurement of thermal conductivity

2.3.1 Description

For the direct measurement of the thermal conductivity, more difficult experiment had to be implemented. As this experiment is way more time demanding than the measurement of RRR, only ISI 1 braid was measured. In comparison with IPE braid it has not only higher thermal conductivity (higher RRR), but also the diameter of one braid wire is approximately 2.5 times smaller ($70\,\mu$m). Thickness of the wire is an important factor influencing the vibration transfer through the braid. Mainly because braid can be used in its unraveled form where less vibrations are transfered, but the cooling power transfer remains the same as in its twined form.

For this experiment a device for measuring mutual emissivity of surfaces was used [14]. One wire of the braid is connected to the upper hot plate at temperature T_R on one end and to the bottom cold plate at temperature T_A on the other end, see Fig. 2.1. The temperature T_B is held almost constant at 4.2 K via thermal anchor to liquid helium. When the upper plate is heated up there is the same heat flux trough the braid and trough the calibrated stainless steel thermal resistor. Thanks to the resistor calibration, from the temperature difference $T_A - T_B$ on the ends of the thermal resistor the heat flux through the braid and the resistor is determined.

The experiment was firstly simulated in program Kryom [15] to determine the best length of the braid. The simulation was needed to determine expected temperatures at the bottom plate T_A and thermal anchor T_B at different temperatures of the top plate T_R for given guessed length of the braid wire. The difference $T_A - T_B$ has to be big enough to be measured with reasonable precision, but small enough to satisfy the calibration conditions. Radiative heat transfers between the plates and

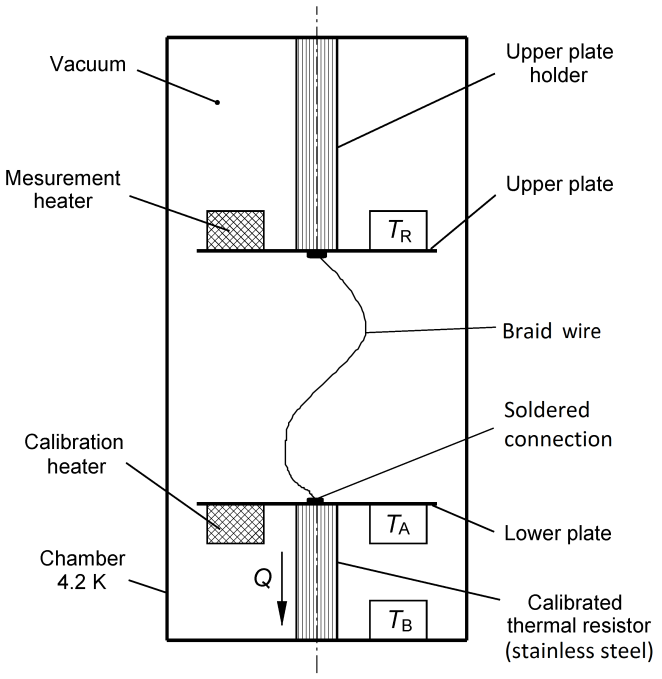

Fig. 2.1: Scheme of the apparatus used for thermal conductivity measurement

between braid and surrounding were not included. Both of these heat transfers were subsequently calculated. Together they form maximally only 5% of the heat flux and only at the highest temperatures, so it is reasonable to neglect them. Further explanation of the measurement method, apparatus and calibration is in section 3.5.

2.3.2 Results

Measured data of thermal conductivity of ISI 1 braid are plotted in Fig. 2.2 (linked circles) and compared with calculated thermal conductivity for different values of RRR in software Cryocomp [6].

Measured thermal conductivity in temperature range above 30 K is in a good agreement with calculated value of RRR = 64 that was determined by previous experiment discussed in section 2.2. A difference between curves under 30 K can be explained by higher uncertainty of as much as ± 0.5 K in temperature measurement around 25 K due to used Lake Shore diode thermometers [16]. This uncertainty is caused by a sharp knee region in fitting calibration curve of diode thermometer in 20 K - 25 K temperature range, from which temperature of the thermometer is determined. A verifying measurement after heating it up to 60 K and cooling it back to 16 K was performed on the same sample (linked triangles in Fig. 2.2).

The measurement of thermal conductivity of the braid was done once again later with much smaller uncertainty to verify the functionality of a newly developed

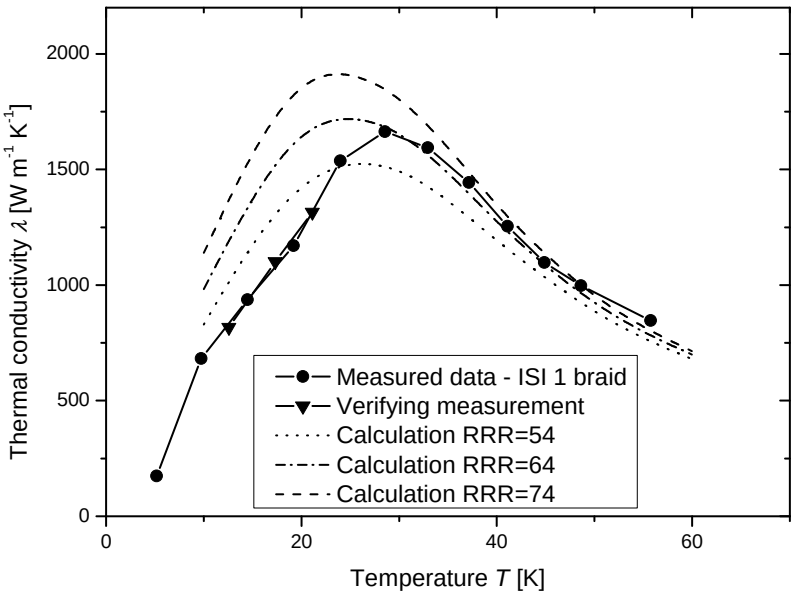

Fig. 2.2: Measured thermal conductivity of ISI 1 braid compared with calculated values for various RRR

apparatus for measuring contact heat conductivity. See more in chapter 3.

3 CuCrZr ALLOY FOR SAMPLE HOLDER

3.1 Introduction

The sample holder of LT-STM should be designed from a material with high thermal conductivity and simultaneously high tensile strength. These two parameters, often needed in cryogenic devices, usually rule out each other. High purity copper is a good conductor, but it's tensile strength limitations are well known. On the contrary, a compromise between thermal conductivity and material strength can be found with precipitation hardened copper alloys with about 2 % of the amount dopants such as Cr, Be or Zr. Higher concentration of dopants lowers the thermal conductivity significantly.

Commercially available CuCrZr alloy is widely used in electrical and thermal conducting field (e.g. as electrodes of resistance welding, trolley wires of electric railway, electrical brushes) for it's good mechanical properties and high conductivity [17]. Furthermore, material characteristics at higher temperatures are well known as CuCrZr is often used for plasma facing parts in devices for fusion energy research [18]. Unfortunately, low temperature characteristics of such alloys are often unknown or unpublished. Hence, based on a published article [19], an alloy CuCrZr was chosen to be explored for its potential use in LT-STM apparatus as a material for sample holder and perhaps heat exchangers.

To estimate the yield strength of this alloy, Brinell hardness was measured. Thermal conductivity was both measured directly and also calculated from electrical resistivity to verify Woodcrafts modification [10] of the equations given by Hust [9] mentioned in section 1.2.3. Results were published in journal Cryogenics [7].

3.2 Samples

3.2.1 Composition

Some material characteristics of CuCrZr alloy are listed in standards (e.g. UNS 18200), but these standards permit very wide range of composition tolerance (e.g. 0.3 % - 1.2 % for Cr), i.e. manufacturer's certificate of composition is needed. Hence, commercially available alloy in shape of 0.8 mm thick cold rolled sheet was purchased from supplier KOVOHUTĚ ROKYCANY, a. s. able to issue such composition certificate. The composition is shown in Tab. 3.1.

Tab. 3.1: Composition of the CuCrZr samples material

Cr	Zr	Fe	Si	Cu
0.71 %	0.23 %	0.01 %	0.02 %	Balance

3.2.2 Thermal treatment

Because CuCrZr alloys belong to precipitation hardening alloys, their final properties depend strongly on the course of the heat treatment. The effects of different heat treatment on these alloy's properties can be found in literature [18, 20, 21]. Based on literature typical annealing and hardening process was executed on some samples. The samples were canned into a thin wall stainless steel tube filled with gaseous helium before heating up to prevent oxidation. Thermally threated samples were all solution annealed at 980 °C for 1.5 hours and cooled down with water. Some of the samples, named CuCrZr-H, were then hardened at 480 °C for 5 hours and slowly cooled down at ambient air. Non-threated samples named CuCrZr-X were studied as they came from supplier. The samples which were annealed only are named CuCrZr-A. The thermal treatment processes are summarized in table Tab. 3.2 and sample marking in Tab. 3.3.

Tab. 3.2: Thermal treatment processes

	Annealing	Hardening
Temperature	980 °C	480 °C
Time heated up	1.5 hours	5 hours
Cooling down	rapid in water	slow in ambient air

Tab. 3.3: Sample marking

	Annealing	Hardening
CuCrZr-X		
CuCrZr-A	✓	
CuCrZr-H	✓	✓

3.2.3 Shaping

Supplier provided a cold rolled sheet of 0.8 mm in thickness. The samples in shape of strips of 0.8 mm in width and 200 mm in length were prepared by shearing. To be

certain that mechanical deformation caused by shearing does not affect the properties of material, one reference sample of each thermally threated type was prepared by sawing. However, no significant difference in material characteristics was found.

3.3 Mechanical properties

For constructional use of CuCrZr alloy knowledge of hardness and material strength is necessary. Measurements of yield strength might be quite cumbersome, but measurement of hardness is fairly simple. Thanks to the relation between strength and hardness [22] an approximate value of the yield strength can be determined from material hardness.

T. Králik (co-author [7]) measured the Brinell hardness of samples by indenting the test material with a 2.5 mm diameter hardened steel ball subjected to total load of 42.25 kg with 10 kg of preload. The diameter of the indentation was measured with a low powered optical microscope. The diameter measurement was checked with confocal microscope on some samples. Hardness of some samples was also done at the Institute of Material Science and Engineering at Brno University of Technology to verify the results. A good match was found.

The data show that, as expected, annealing significantly lowers hardness. Cold rolling of the alloy after hardening by manufacturer explains the fact that hardness of non-treated samples is almost twice as high as for hardened samples. Results are shown in a table Tab. 3.4.

Tab. 3.4: Brinell hardness of CuCrZr samples

		CuCrZr-X	**CuCrZr-A**	**CuCrZr-H**
Brinell hardness	[−]	236	56	128

The models for determination of yield strength from material hardness are mostly empirical and quite complicated. Commercially used hardened CuCrZr alloy AMPCOLOY 972 [23] with corresponding composition shows similar Brinell hardness (HRB = 120 − 150). The manufacturer states the value of yield strength for this alloy as 410 MPa. Similar strength is assumed for the tested hardened CuCrZr-H. Non-threated and annealed CuCrZr do not have practical use in cryogenic devices and strength determination is not necessary. Alloy after annealing is not in a stable state and material characteristics of such alloy may vary with time and thermal cycling. Material characteristics of cold rolled alloy may change localy with soldering at higher temperatures.

3.4 Measurement of electrical resistivity

As in section 2.2 electrical resistivity was measured on each sample at 295 K and at 4.2 K. From these values RRR was calculated. Results can be found in Tab. 3.5. From the values of RRR the thermal conductivity was calculated with freely available program [11] developed by A. Woodcraft and is plotted in Fig. 3.4 together with measured data from direct measurement of thermal conductivity. There is almost no difference in calculated conductivity between hardened (CuCrZr-H) and non-treated alloy (CuCrZr-X), but conductivity of annealed alloy (CuCrZr-A) is substantially lower.

Tab. 3.5: Measured electrical resistivity and RRR of CuCrZr samples

		CuCrZr-X	**CuCrZr-A**	**CuCrZr-H**
Electrical resistivity ρ at 295 K	[Ω m]	2.30×10^{-8}	5.26×10^{-8}	2.22×10^{-8}
Electrical resistivity ρ at 4.2 K	[Ω m]	4.56×10^{-9}	3.61×10^{-8}	4.48×10^{-9}
RRR	[−]	5.04	1.46	4.95

3.5 Direct measurement of thermal conductivity

3.5.1 Measurement method

For measuring thermal conductivity of CuCrZr samples a new apparatus for contact conductivity measurements was implemented, see Fig. 3.1 and [7]. It is based on the device for measuring mutual emissivity discussed in section 2.3.1 with two major differences:

- Due to much higher heat fluxes through the sample (caused by bigger dimensions than in the case of braid wires) a tube from a high conductive material was used as a thermal resistor between temperatures T_A and T_B.
- For the measurements of contact conductivity, force can be applied to the top plate to simulate mechanical load of the contact. This aspect is further discussed in section 4.5.

The ends of the sample are soft soldered to flanges joined to two plates with temperatures T_R and T_A regulated by heaters and measured by Cernox^{TM} [24] thermometers. Negligible temperature difference across these contacts is assumed. The lower plate is in thermal contact with calibrated thermal resistor (made of CuCrZr) with much higher thermal conductivity than that of the sample. There is also a radiation shield between the upper and the lower plate with an orifice for the sample to lower the radiative heat flux. This whole setup is put inside a vacuum shell

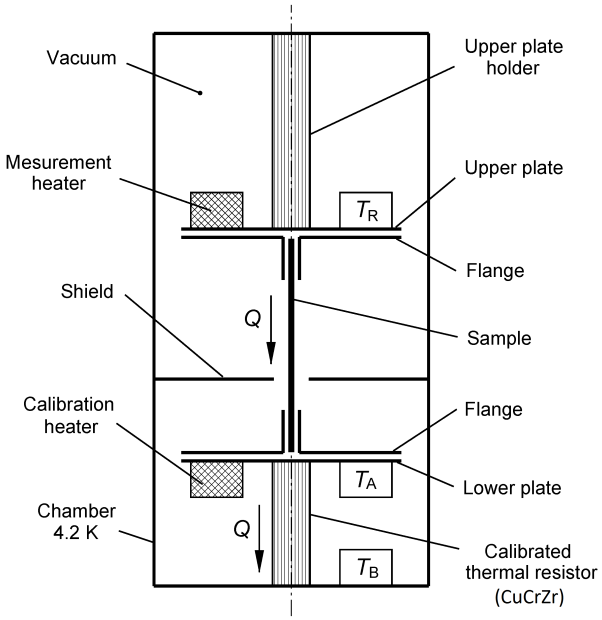

Fig. 3.1: Apparatus for measuring contact thermal conductivity

submersed into LHe in Dewar vessel. The thermal contact with LHe is ensured by conductive copper flange connected to thermal resistor.

Thermal resistor

Because much higher heat fluxes were estimated than in the case of emissivity measurements, a thermal resistor with higher thermal conductivity had to be implemented. It is important to choose thermal conductivity of the resistor properly, because heat flux through the sample is calculated from the temperature difference $T_A - T_B$ at the ends of the resistor. If the conductivity is too high, this temperature difference will be small and measured with significant error. On the other hand, if the conductivity is too low, the temperature difference will be too big and the conditions needed for calibration of the resistor will not be fulfilled.

CuCrZr was chosen as a material for this thermal resistor especially for its high stability of thermal conductivity under thermal cycling (in comparison with that of e.g. copper) and high thermal conductivity (in comparison with that of e.g. thermally stable stainless steel). The dimensions of the thermal resistor were optimized for the right conductivity with software Kryom [15]. The final dimensions of the tube were chosen to be 9.2 mm/7.8 mm in diameter and 15 mm in length.

Thermal resistor was calibrated without the sample by stepwise heating of the lower plate to the temperature T_A with calibration heater. The dependence of heat flux Q on the temperature difference $T_A - T_B$ was measured. Later, when samples

are measured, heat flux Q is calculated from the values T_A and T_B. From this heat flux the thermal conductivity of the sample can be calculated. Further explanation of this method and error analysis can be found in [7].

Test measurements

Arranged new contact conductivity apparatus was verified by test measurement of heat conductivity of stainless steel. Stainless steel is a very common material for cryogenic devices, which low temperature properties are well documented and do not depend much on a composition and previous treatment. For this reason, thermal conductivity of a stainless steel 304 sample in shape of a rod with 1.98 mm in diameter and 42.5 mm in length was measured in the temperature range from 4.2 K to 300 K. Gained data were then compared with the cryogenic thermal conductivity database of National Institute of Standards and Technology [25] and are plotted in Fig. 3.2. A good agreement can be seen within the whole temperature range. The maximum deviation from the reference values does not exceed 10 % under 10 K and 5 % in temperature range over 10 K.

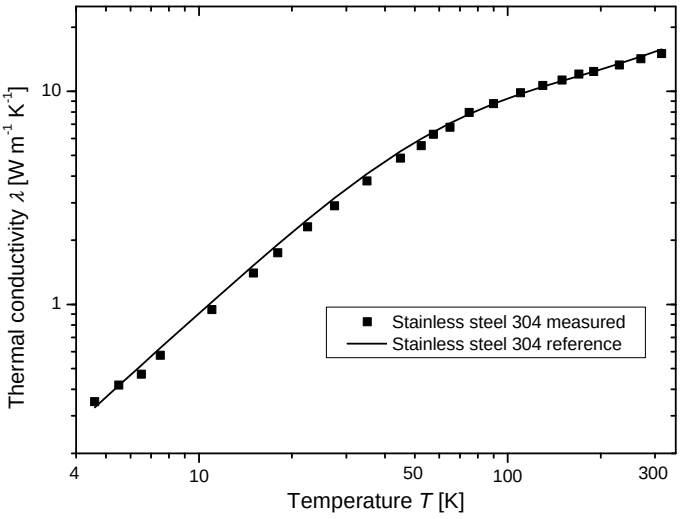

Fig. 3.2: Test measurement: Comparison of measured and reference data for 304 stainless steel

Stainless steel is a material with relatively low thermal conductivity. To refine our previous measurement mentioned in section 2.3 and to test the apparatus on a high conductivity sample, ISI 1 braid was measured again with this apparatus. The results can be seen in Fig. 3.3. Surprisingly, a good correlation with the calculated value of thermal conductivity for RRR = 54 can be seen even though the determined RRR value from previous experiment (section 2.2) is 64, see results for ISI 1 braid in Fig 2.1. That might be caused by the deformation of the braid sample during manipulation in experiment from section 2.2.

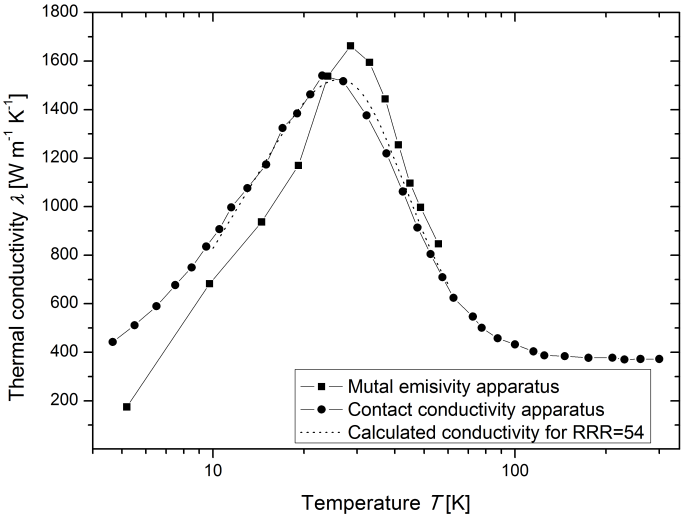

Fig. 3.3: Test measurement: Thermal conductivity of ISI 1 braid

3.5.2 Results

After the testing of the apparatus, the measurement of variously threated CuCrZr samples (CuCrZr-X, CuCrZr-A, CuCrZr-H) could be implemented. The measured results are plotted in Fig. 3.4 with the previously calculated values of thermal conductivity from RRR measurement mentioned in section 3.4.

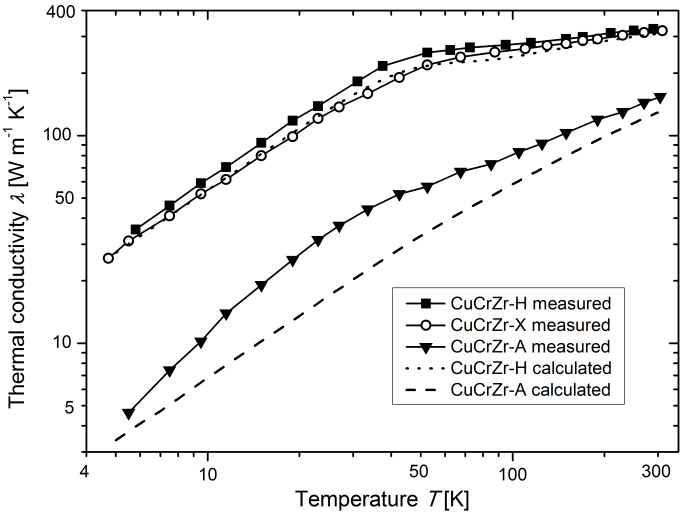

Fig. 3.4: Thermal conductivity of variously thermaly threated CuCrZr alloys

As expected from the RRR measurement, thermal conductivity of CuCrZr after annealing is significantly lower than after hardening process. Hardening seems to make no difference in conductivity comparing to non-threated alloy. The difference between measured and calculated data for annealed alloy are probably caused by uncertainty of the calculation model. Wooodcraft [19] states that the calculation

model for copper alloys is reasonably accurate for RRR down to 2. Calculation of hardened CuCrZr-H is above this limit (RRR = 4.95) unlike annealed CuCrZr-A (RRR = 1.46).

4 SPHERICAL CONTACT SUPPORT

4.1 Introduction

To ensure low temperature of the sample holder in LT-STM, the proper isolation from the table at ambient temperature is necessary. That is a difficult problem, because the difference of the temperatures of the sample and of the table is over 250 K. J. Nekula proposed a STM design at his diploma thesis [1] where cryogenic cooling is mentioned. His design of the table with the sample holder and the scanner is shown in Fig. 4.1.

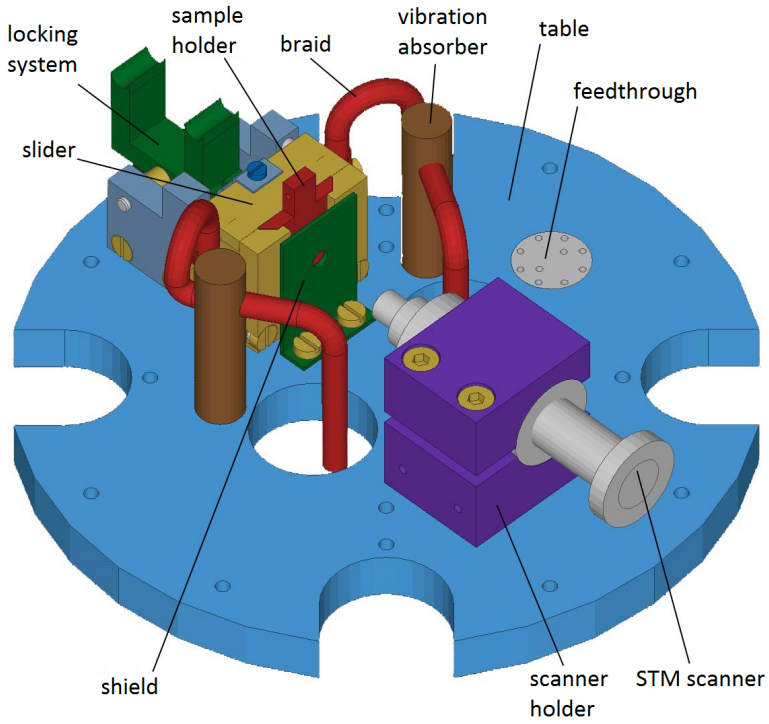

Fig. 4.1: Proposed design by J. Nekula [1]

Hoverer, this draft does not respect many of the principles for designing cryogenic apparatus. Cooling to less than even 100 K with reasonable mass flow rate of He would not be possible in this setup. To give one example, the radiation from warm surfaces are not taken into consideration at all, even though its ratio to the other parasitic heat fluxes to the sample is not negligible. The detail of the sample holder can be seen in Fig. 4.2 with highlighted cold parts. The whole insulation of the cold parts would only be realized by ceramic O-rings with low thermal conductivity. Such a setup would have enormous heat losses, thus a different solution had to be found.

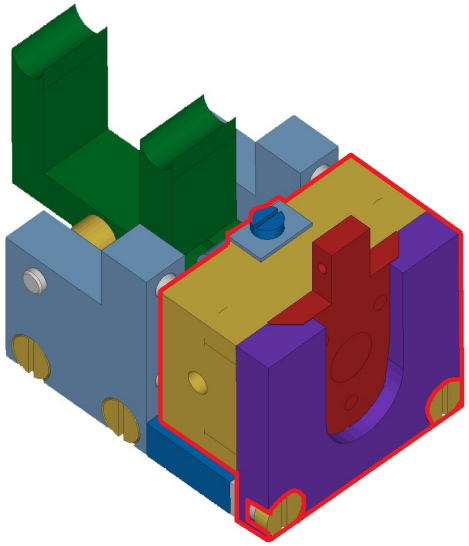

Fig. 4.2: Detail of the sample holder from Fig 4.1 with highlighted cold parts [1]

P. Hanzelka (author of [7]) designed a support of the sample holder with spherical contact, preventing the enormous heat leaks to the sample (Fig. 4.3 b). The design of the support feature was studied both theoretically and experimentally on two main prototypes.

4.2 Design

Three main characteristics of the support feature have to be accomplished:

- As low thermal conductivity as possible
- Sufficient mechanical stability
- Ultra-high vacuum compatibility

The criteria were met with the design of the support with the spherical contact. Under mechanical load, there is a small contact surface on the spheres that acts as a thermal resistance [3].

Two designs were studied: version with a single glass sphere (Fig. 4.3 a) and version with four spheres forming a pyramid (Fig. 4.3 b). Even though lower thermal conductivity was expected for the support with pyramid setup, the support with single sphere was also studied, because there was some doubt about the mechanical stability of the pyramid setup. The forces at the supports during sample manipulation are rather high, due to the fact that the sample exchange has to be done with a vacuum cell manipulator called *wobble stick*. The supports are connected with sample holder via a screw thread at the top and there is another threaded hole at the bottom to connect the support with the table.

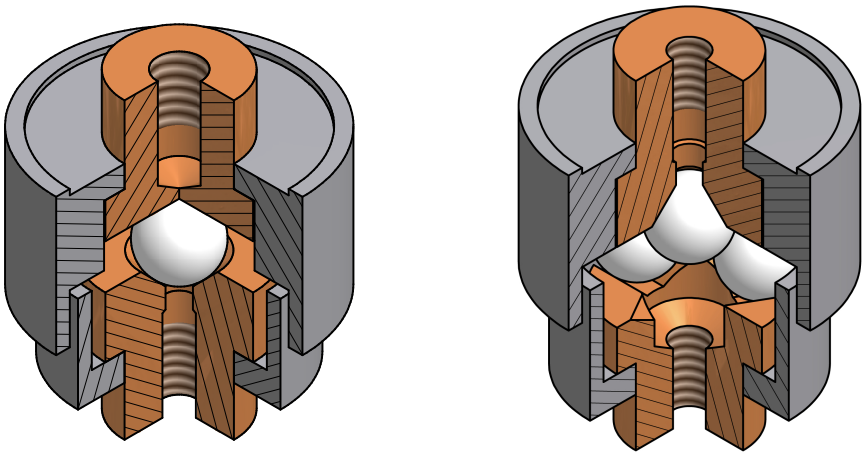

a) b)

Fig. 4.3: Support with spherical contact. Single sphere setup (a) and the pyramid setup (b).

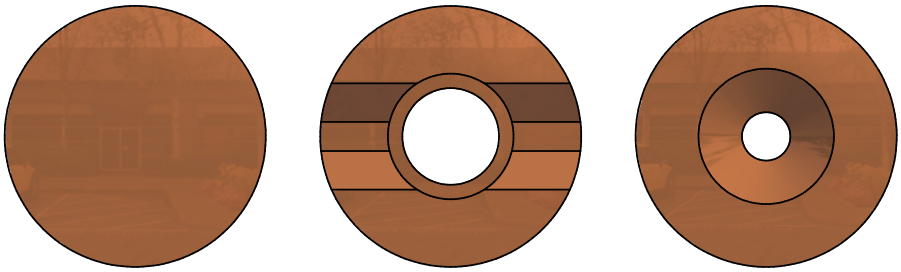

a) b) c)

Fig. 4.4: Three types of seats in contact with the sphere at the top of the pyramid

For proper fixation of the sample holder four of the supports are needed. Three from the bottom and one from the top of the holder. The support from the top is necessary to set a defined mechanical load and prevent the movement of the sample holder in vertical direction.

It is essential that the sample holder has zero kinematic degrees of freedom towards the table. On the other hand the setup has to allow thermal contraction of the sample holder. Otherwise high mechanical stress occurs between the spheres, and their contact and relative position are not defined.

For this reason the seats that are in contact with the sphere at the top of the pyramid are in three types of shapes allowing either full plane (Fig. 4.4 a), linear (Fig. 4.4 b) or no motion of the top sphere (Fig. 4.4 c). For the bottom supports all three types are used and for the top support type a) is used. That allows all the spheres to sit in the proper position.

4.3 Material selection for the spheres

To lower the conductivity of the setup the right material for the spheres had to be chosen. The material had to have very low thermal conductivity, high Young's modulus of material to ensure small contact surfaces and it has to be ultra high vacuum compatible.

There are many plastic materials with very low thermal conductivity, but usually they do not fulfill the condition of ultra high vacuum compatibility. Often they have too low melting point, so they would not withstand baking out of the apparatus and their outgassing rates are also relatively high. Surprisingly, thermal conductivity of ceramic materials and glass varies from one material to another. For example thermal conductivity of sapphire at about 50 K is even better than that of very pure copper. On the other hand synthered ceramics such as Macor or glasses such as Pyrex show very low thermal conductivity. The conductivity changes also with the state of the material. For example, the conductivity ratio for Quartz (SiO_2) in crystalline state and glass state is 5 orders of magnitude at 10 K. Thermal conductivity of all the materials mentioned above is plotted in Fig 1.1.

The spheres 2.5 mm in diameter made of Pyrex glass (with other commercial name Simax) were chosen for the purpose of the low conductive supports, because this glass fulfills all the mentioned criteria. Pyrex is a commercially available borosilicate glass with low thermal conductivity and high Young's modulus.

4.4 Heat flux calculation

Before the measurement of heat fluxes through the support could be implemented, approximate thermal conductivity had to be calculated to determine what heat fluxes to expect during the experiment. Only the version of support with one sphere was calculated due to its simplicity. The contact surfaces increase with mechanical load at the sphere, thus thermal conductivity is force dependent. The contact surface area was calculated using Hertz equations, see section 1.3. For this contact area heat flux through the sphere was calculated using calculation model described in [26]. Thermal resistance was assumed only on the contact surface between the sphere and the top plate, because the resistance in the other areas of the setup is much lower.

This method gives reasonable estimate of the heat fluxes, but naturally it is in no way as accurate as measurements. More detailed simulation using finite elements method is necessary for proper calculation model.

The results of calculation are plotted in Fig. 4.5 with the measured data as it is described in section 4.5.

4.5 Measurement

The dependence of heat flux on mechanical load on supports was measured using contact conductivity apparatus discussed in section 3.5. This apparatus allows applying various forces at the upper plate at temperature T_R and even changing them during the experiment when everything is cooled down. The dependence of heat flux on applied force was measured for the temperature of upper plate T_R at 300 K, 200 K, 100 K and 50 K. The results are plotted in Fig. 4.5. An assumption that the pyramid support has lower conductivity was confirmed. It is at least twice as low as single sphere support in the whole temperature range. An agreement between calculated and measured heat fluxes was found for the T_R lower than 300 K. Calculated heat flux is less then a half of the measured value for $T_R = 300$ K. This difference is most likely caused by thermal radiation inside the support that is not included in calculation model. Thermal radiation is proportional to fourth power of temperature.

4.6 Conclusion

The measured heat fluxes are relatively low. Naturally, for the purpose of the sample holder insulation the measured heat fluxes for temperature $T_R = 300$ K (Fig. 4.5) are the most important. Heat flux through the pyramid setup does not exceed 20 mW for mechanical load under 3 N, that is about 2.5 times lower than in case of single sphere setup. To mention another variant that was coming into consideration for comparison (table at 300 K and sample at 30 K are assumed): heat flux through a stainless steel tube with 0.15 mm thick walls, 8 mm in diameter and 60 mm in length, is about 15 times higher than that of pyramid setup. Not to mention the bulkiness of the whole setup and vibration problems that occur when using such a long rods.

Mechanical stability of the pyramid setup seems to be sufficient enough and this setup will most likely be used in LT-STM design. After further successful computer simulations in software COMSOL by finite elements method, the design might be ready for application.

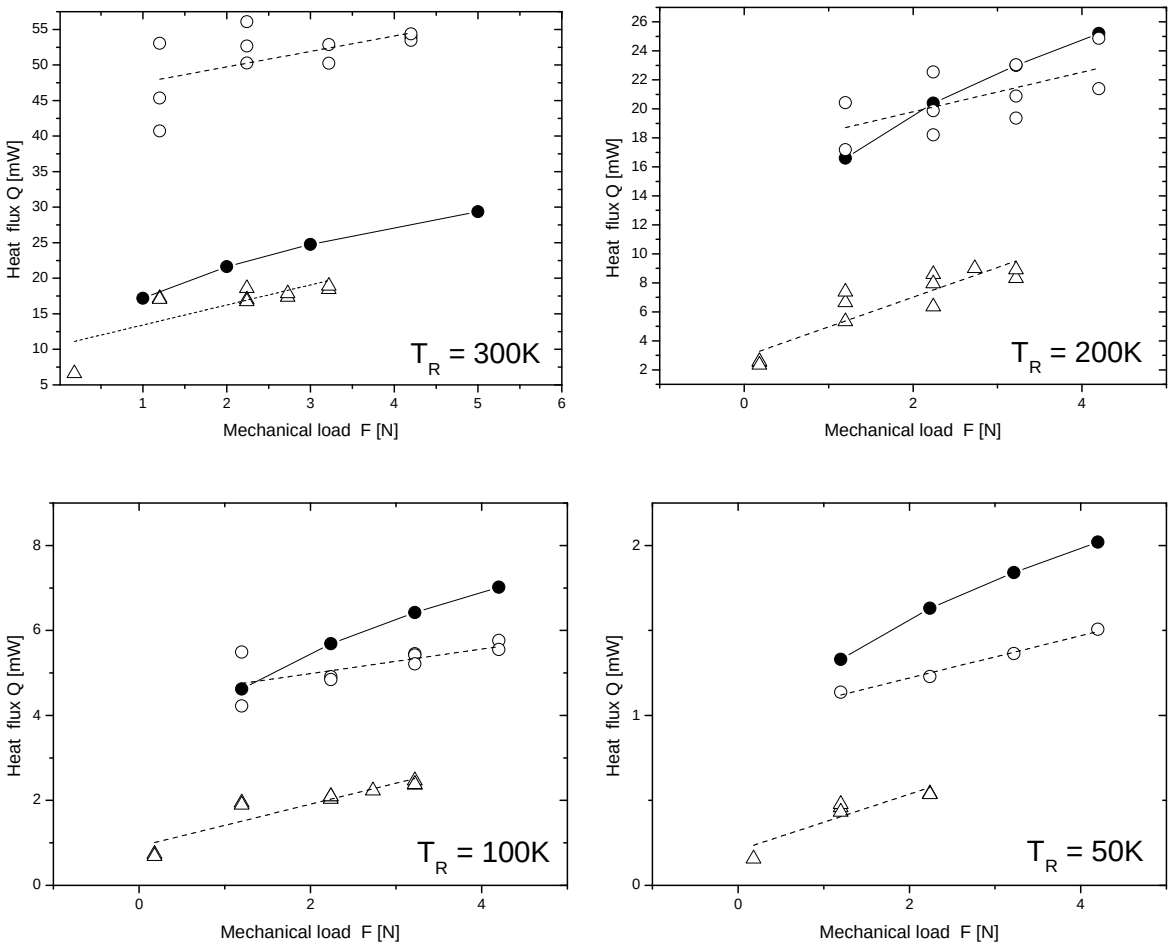

Fig. 4.5: Measured and calculated thermal conductivity of spherical supports. Values for calculated thermal conductivity of a single sphere setup are plotted with sign •. The measured values for pyramid setup are plotted with sign △ and for the single sphere setup with sign ○.

5 CONCLUSIONS

For the purpose of the LT-STM microscope design, thermal and mechanical characteristics of various materials were studied with respect to their use in three main features of the LT-STM (Fig. 1):

- Copper braids
- Sample holder
- Low conductive supports

Dependence of thermal conductivity on temperature in range from 4 K to 300 K of two types copper braids, named ISI and IPE, was determined by measuring electrical resistivity together with Wiedeman-Franz-Lorentz Law and by further direct measurement of thermal conductivity (Fig. 2.2). ISI braid turned out to be more suitable for use in LT-STM due to its higher thermal conductivity and smaller diameter of its wires (lower transfer of vibrations).

CuCrZr alloy was studied for potential use for parts where high material strength and simultaneously high conductivity is needed (e.g. sample holder, heat exchangers). Brinell hardness and thermal conductivity of variously thermally threated samples was measured (section 3.3). Dependence of thermal conductivity on temperature in rage from 4 K to 300 K was determined both by measuring electrical resistivity and by direct measurement. Measured data (Fig. 3.4) proved the usability of this material in LT-STM especially for sample holder. Studied mechanical and thermal properties of this alloy were published in journal Cryogenics [7].

For thermal isolation of the sample holder from the table, a support with contact of glass spheres was developed (Fig. 4.3). Mechanical stability of the supports was tested and thermal conductivity was studied both theoretically and experimentally (section 4).The results show (Fig. 4.5), that this design is suitable for use in situations, where contact with very low thermal conductivity is needful. On the base of these results the support is supposed to be used in LT-STM.

Determination of thermal conductivity of these components can be used for various other cryogenic applications and are one of the first steps to build flow cryogenic cryostat for the STM at the Institute of Physical Engineering. As a next step an experimental vacuum cell will be designed to test the cooling power of the cryostat and to determine its dependence on He flow rate. The work was done within the Group of Cryogenics and Superconductivity at Institute of Scientific Instruments and will conctinue hereafter.

BIBLIOGRAPHY

[1] NEKULA, J. *Návrh rastrovacího tunelovacího mikroskopu STM*. Brno, 2004. 59 p. Diplomová práce. Vysoké Učení Technické, Fakulta Strojního Inženýrství.

[2] EKIN, J. W. *Experimental Techniques for Low-Temperature Measurements*. Oxford : OUP, 2006. 704 p. ISBN 978-0198570547.

[3] WEISEND, J. G. *Handbook Of Cryogenic Engineering*. Philadelphia : Taylor and Francis, 1998. 504 p. ISBN 978-1560323327.

[4] BARRON, R. F. *Cryogenic Heat Transfer*. 1st ed. Philadelphia : Taylor & Francis Ltd, 1999. 374 p. ISBN 1560325518.

[5] JELÍNEK, J.; MÁLEK, Z. *Kryogenní technika*. Praha : STNL, 1982. 354 p.

[6] The CryoComp package (Version 3.0) [Software]. (1997). Eckels Engineering Inc. Florence, SC, USA. URl: `http://www.eckelsengineering.com`

[7] HANZELKA, P., et al. Thermal conductivity of a CuCrZr alloy from 5 K to room temperatures. *Cryogenics*. 2010, Vol. 50, Issues 11-12, p. 737-742.

[8] HRIVNÁK, Ľ., et al. *Teória Tuhých Látok*. 2nd ed. Bratislava : Veda, 1985. 578 p.

[9] HUST, J. G.; LANKFORD, A. B. Thermal conductivity of aluminium, copper, iron and tungsten from 1 K to the melting point. Colorado: National Bureau of Standards; 1984. NBSIR 84-3007.

[10] WOODCRAFT, A. L. Predicting the thermal conductivity of aluminium alloys in the cryogenic to room temperature range. *Cryogenics*. 2005, Vol. 45, Issue 6, p. 421-431.

[11] WOODCRAFT, A. Copper thermal conductivity calculator [online]. 2009 [cit. 2011-05-15]. Copper and dilute copper alloy thermal conductivity calculator. URL: `http://reference.lowtemp.org/cucalc.html`.

[12] BUDYNAS, R.G.; NISBETT, J.K. *Shigley's Mechanical Engineering Design*. 8th ed. [s.l.] : Budynas-Nisbett, 2006. 1088 p. ISBN 0073312606.

[13] BAHRAMI, Majid. *Modeling of Thermal Joint Resistance for Sphere-Flat Contacts in a Vacuum*. Waterloo (CA), 2004. 246 p. Diploma thesis. University of Waterloo.

[14] KRALIK, T., et al. Device for measurement of thermal emissivity at cryogenic temperatures. *In Proceedings of IIR conference*. Praha : ICARIS, 2004. p. 23-29. ISBN 2-913149-33-2, ISSN 0151-1637.

[15] HANZELKA, P., VEJCHODA, I. (1998). Kryom (Version 3.3). [Software]. Institute of Scientific Instruments, Brno, CZ.

[16] Lake Shore Cryotronics, Inc. [online]. 2011 [cit. 2011-05-24]. Cryogenic Temperature Sensors - Silicon Diodes - Product Overview. URL: `http://www.lakeshore.com/temp/sen/sd.html`.

[17] ZHANG, Y.; ZENG, J.; ZHUANG, Y. Tribological Properties of Al2O3/CuCrZr Composites. *Tribology Letters*. 2005, Vol. 20, Num. 2, p. 163-170. ISSN 11249-005-8311-1.

[18] LIPA, M., et al. The use of copper alloy CuCrZr as a structural material for actively cooled plasma facing and in vessel components. *Fusion Engineering and Design*. 2005, Vol. 75-79, p. 469-473.

[19] WOODCRAFT, A. L. . Zirconium Copper - a New Material for Use at Low Temperatures?. *Proceedings of the 24th International Conference on Low Temperature Physics* [online]. 2005, [cit. 2011-05-15]. URL: `http://reference.lowtemp.org/woodcraft_zrcu.pdf`.

[20] MEROLA, M., et al. Influence of the manufacturing heat cycles on the CuCrZr properties. *Journal of Nuclear Materials*. 2002, Vol. 307-311, p. 677-680.

[21] IVANOV, A., et al. Effect of heat treatments on the properties of CuCrZr alloys. *Journal of Nuclear Materials*. 2002, Vol. 307-311, p. 673-676.

[22] TABOR, D. The physical meaning of indentation and scratch hardness. *British Journal of Applied Physics*. 1956, Vol. 7, Num. 5, p. 159-166.

[23] AMPCO METAL [online]. 2011 [cit. 2011-05-26]. AMPCOLOY 972. URL: `http://www.ampcometal.com/cz/index.php?page=a972ext`.

[24] Lake Shore Cryotronics, Inc. [online]. 2011 [cit. 2011-05-16]. Cryogenic Temperature Sensors - Cernox - Product Overview. URL: `http://www.lakeshore.com/temp/sen/crtd.html`.

[25] RADEBAUGH, R., et al. *NIST, Cryogenics Technologies Group* [online]. 2010 [cit. 2011-05-15]. Material Properties. URL: `http://cryogenics.nist.gov/MPropsMAY/materialproperties.htm`.

[26] KUMAR, S. S.; ABHILASH, P. M.; RAMAMURTHI, K. Thermal Contact Conductance for Cylindrical and Spherical Contacts. *J. Heat and Mass Transfer*. 2004, vol. 40, No.9, p. 679-688.

[27] POBELL, F. Matter and Methods at Low Temperatures. 3rd ed. Berlin : Springer, 2007. 461 p. ISBN 13 978-3-540-4636-6.

[28] ROSENBERG, H. M. *The Solid State*. 3rd ed. Oxford : OUP, 1988. 326 p. ISBN 978-0-19-851870-9.

LIST OF SYMBOLS, PHYSICAL CONSTANTS AND ABBREVIATIONS

e elementary charge [C]

E Young's modulus [Pa]

F force [N]

k_{B} Boltzman constant $[\mathrm{m^2\,kg\,s^{-2}\,K^{-1}}]$

L length [m]

L_0 Lorentz number $[\mathrm{W\,\Omega\,K^{-2}}]$

p pressure [Pa]

R radius [m]

S cross-section area $[\mathrm{m^2}]$

T temperature [K]

t time [s]

q heat [J]

Q heat flux [W]

λ heat conductivity $[\mathrm{W\,K^{-1}\,m^{-1}}]$

ν Poisson's ratio [-]

σ electrical conductivity $[\mathrm{S\,m^{-1}}]$

ρ electrical resistivity $[\mathrm{\Omega\,m}]$